24th COBEM - 2017

24[th] ABCM International Congress of Mechanical Engineering
December 3-8, 2017, Curitiba, PR, Brazil

COBEM-2017-0478 NUMERICAL SIMULATION OF THE NEUTRAL ATMOSPHERIC SURFACE LAYER FLOW OVER REAL TERRAIN: THE ASKERVEIN HILL CASE

William Correa Radunz
Federal University of Rio Grande do Sul, Graduate Program in Mechanical Engineering (PROMEC), R. Sarmento Leite, 425, 90050-170, Rio Grande do Sul, Brazil
william.radunz@ufrgs.br

Adriane Prisco Petry
Federal University of Rio Grande do Sul, Department of Mechanical Engineering (DEMEC), R. Sarmento Leite, 425, 90050-170, Rio Grande do Sul, Brazil
adrianep@mecanica.ufrgs.br

Abstract. *The demand for more accurate numerical wind flow models, used for predicting the micro-scale wind climate of a proposed wind farm, requires extensive validation against high-quality atmospheric-scale experiments. In the present study, the open-source platform OpenFOAM is used to simulate the atmospheric surface layer wind over one of such experiments, namely the Askervein hill. Consistency was ensured by proper choice of the $k-\epsilon$ model constants, wall-functions and inflow conditions, which means a sustainable fully-developed boundary layer is achieved. Three choices of the constant C_μ were evaluated with four grids so as to assess the sensitivity. Generally, the models were able to predict the wind behavior but overestimated the wind speed in the lee, whilst underpredicted the turbulence kinetic energy. The Atmospheric formulation performed slightly better than the other models, but still resulted in unacceptable errors in wind speed.*

Keywords: *Wind flow, OpenFOAM, Askervein Hill*

1. INTRODUCTION

Wind power plants projects are highly sensitive to the wind resource uncertainties, owing to the fact that the revenues are based on production estimates. As it is unfeasible due to technical and economical restrictions to place a number of met masts high enough to obtain a figure of how the wind resource varies across the site, numerical wind flow models may be used to simulate the local wind climate.

The complexity of these models ranges from simpler linear models like WAsP (Wind Atlas Analysis and Application Program), based on Jackson and Hunt (1975), and Computational Fluid Dynamics (CFD). The linear models tend to over estimate the wind speed at the top of elevations since they assume attached flow and small terrain perturbations. CFD, however, is theoretically capable of capturing non-linear flow phenomena as separation and recirculation through the Reynolds-Averaged Navier-Stokes (RANS) approach.

Since most of the RANS turbulence models were created under an engineering-scale perspective, meaning that scales were in the order of millimeters to meters, it was necessary to adapt the model constants, boundary conditions and wall-functions to the kilometer-scale engineering of micro-scale meteorology. The demand for model inter-comparison and validation led to the Askervein Hill project (Taylor and Teunissen, 1987), which was a major endeavor for obtaining and assessing reliable micro-scale wind data. According to Taylor and Teunissen (1987), the hill has a number of features that make it valuable for numerical model evaluation which includes its elliptical shape, a pronounced main wind direction and the fact that it is nearly isolated.

The Askervein Hill has been extensively simulated using a number of models, ranging from simpler linear models, spectral (Beljaars *et al.*, 1987), RANS (Castro *et al.*, 2003; Balogh *et al.*, 2012) and LES. As a summary on previous results, it can be said that, in general, the models tend to under predict the TKE peak in the lee of the hill and the speed-up at the hill top.

In the present study, the open-source C++ toolbox OpenFOAM is used as the environment for wind flow model development. The library has a number of peculiarities which are inviting for model development, which include the freely-editable state-of-the-art CFD and field operations code. The work presented here includes the modifications of some of the code wall-functions, the methodology for selecting the $k-\epsilon$ turbulence model constants and the evaluation of model sensitivity to the grid and the aforementioned constants. In section 2. the governing equations of the CFD model are presented alongside the inflow profiles and wall-functions. The domain and boundary conditions based on the measurements are discussed in section 3. Results are compared to the measured data and discussed in 4. Conclusions and highlights of this work are found in section 5.

2. GOVERNING EQUATIONS

According to Stull (2017), the ASL is the lowest portion of the ABL and where the surface effects like friction and heat convection have a major effect on the wind speed and other fields, which change substantially with height. One peculiarity of the ASL is that turbulent *momentum* and heat fluxes are somewhat uniform with height, which is why it is also known as constant flux layer. By neglecting the Coriolis force and stratification effects, the lowest 200 m of the ABL can be modeled by the standard $k - \epsilon$ turbulence model which is shown in index notation below

$$\nu_t = C_\mu \frac{k^2}{\epsilon} \tag{1}$$

$$\frac{\partial}{\partial x_i}(U_i k) = \frac{\partial}{\partial x_j}\left[\left(\nu + \frac{\nu_t}{\sigma_k}\right)\frac{\partial k}{\partial x_j}\right] + G_k - \epsilon \tag{2}$$

$$\frac{\partial}{\partial x_i}(U_i \epsilon) = \frac{\partial}{\partial x_j}\left[\left(\nu + \frac{\nu_t}{\sigma_\epsilon}\right)\frac{\partial \epsilon}{\partial x_j}\right] + C_{\epsilon 1} G_k \frac{\epsilon}{k} - C_{\epsilon 2}\frac{\epsilon^2}{k} \tag{3}$$

$$G_k = \nu_t \left(\frac{\partial U_i}{\partial x_j} + \frac{\partial U_j}{\partial x_i}\right)\frac{\partial U_i}{\partial x_j} \tag{4}$$

where ν_t is the turbulence kinematic viscosity, k is the turbulence kinetic energy (TKE) and ϵ its dissipation rate, U is the Reynolds-Averaged wind speed, ν is the kinematic viscosity of the air and G_k is the TKE production term. The standard model constants are the following:

$$C_{\epsilon 1} = 1.44, \quad C_{\epsilon 2} = 1.92, \quad C_\mu = 0.09, \quad \sigma_k = 1.0, \quad \sigma_\epsilon = 1.3 \tag{5}$$

These classic constants are usually modified for micro-scale atmospheric flow simulation since they were adjusted to engineering-scale flows. Richards and Norris (2011) elucidate that C_μ may be adjusted to fit the TKE in the atmosphere, but the turbulent Prandtl number of the dissipation rate ought to be corrected

$$C_\mu = \frac{u_\star^4}{k^2}, \quad \sigma_\epsilon = \frac{\kappa^2}{(C_{\epsilon 2} - C_{\epsilon 1})\sqrt{C_\mu}} \tag{6}$$

Richards and Hoxey (1993) proposed wind speed and turbulence profiles which produce homogeneous flow for the standard $k - \epsilon$ model. Under the assumptions of negligible vertical velocity, constant pressure and constant shear stress, the following set of inflow profiles are a solution to Eqs. (2) and (3)

$$u = \frac{u_\star}{\kappa} ln\left(\frac{z + z_0}{z_0}\right) \tag{7}$$

$$k = \frac{u_\star^2}{\sqrt{C_\mu}} \tag{8}$$

$$\epsilon = \frac{u_\star^3}{(z + z_0)} \tag{9}$$

The set of equations (7-9) has been extensively used in the fields of wind engineering and WRA to produce sustainable boundary layers. The problem, however, is that the value calculated at the near-ground cell center by these standard WFs may not match the inflow profiles and, thus, cause flow inhomogeneity. It is possible, however, to modify the standard WFs and obtain model consistency similarly to authors Parente *et al.* (2011) and Balogh *et al.* (2012). The consistency is achieved by modifying OpenFOAM's *epsilonWallFunction* by adding z_0 to the following equations

$$\epsilon_P = \frac{C_\mu^{0.75} k^{1.5}}{\kappa(z_P)} \rightarrow \frac{C_\mu^{0.75} k^{1.5}}{\kappa(z_P + z_0)} \tag{10}$$

$$G_{k_P} = \frac{\tau_w^2}{\kappa C_\mu^{0.25} k_P^{0.5}(z_P)} \rightarrow \frac{\tau_w^2}{\kappa C_\mu^{0.25} k_P^{0.5}(z_P + z_0)} \tag{11}$$

where the subindex P stands for near-ground cell center. As for the ν_t WF, a consistent version is already implemented in OpenFOAM, namely *nutkAtmRoughWallFunction*.

3. DOMAIN AND BOUNDARY CONDITIONS

According to Taylor and Teunissen (1987), the Askervein hill consists of a nearly elliptical hill which is mostly surrounded by plain terrain but for some orographic features (although they tend not to affect the flow since they are not located upstream). This is shown in Fig. 1. Since the model employed in this paper is devised for neutrally-stratified atmospheric surface layer flows, the run selected from the Askervein project consisted of a very windy day in which the meteorological conditions were nearly neutral. In Taylor and Teunissen (1987) this run is denoted TU-03B.

The inflow conditions used are those described by Eqs. (7-9) and represent a horizontally-homogeneous neutral ASL. The outlet patch was set as constant pressure. The slip condition is applied at the sides an top of the domain. The ground of the terrain is modeled through the use of the fully-rough atmospheric wall-functions (described in section 2.) with a uniform $z_0 = 0.03$ m.

For the generation of the structured computational mesh, the utility *terrainBlockMesher* developed by Schmidt *et al.* (2012) was used. This application allows for splitting the domain in blocks with different grid densities so that more resolution is put into the region of interest. In addition, a very fine and smoothly-growing mesh is required in the lowest 200 m which represent the ASL. One of the grids used is shown in Fig. 2.

The inflow conditions were determined in two steps for the model denominated Fitted. Firstly, the log-law profile (Eq. 7) is fitted to the wind speed data by using non-linear least squares, thus, determining $u_\star$ and z_0, which is shown in Fig. 3. Subsequently, Eq. (8) is fitted to the TKE measurements and the turbulence model constant C_μ is obtained. For the Standard and Atmospheric set-ups, since C_μ is fixed, the reference TKE is calculated through Eq. (8) rather than fitted to the measurements. It may also be seen in Fig. 3 that indeed the Atmospheric TKE profile does not match the data, and the explanation for this approach is related to the consistency between turbulence model, wall-functions and inflow conditions. Since the inflow profiles represent the fully-developed ASL, if the TKE profile were matched to the measurements maintaining the model constant $C_\mu = 0.033$, the inflow conditions would no longer represent equilibrium profiles and would change artificially throughout the domain.

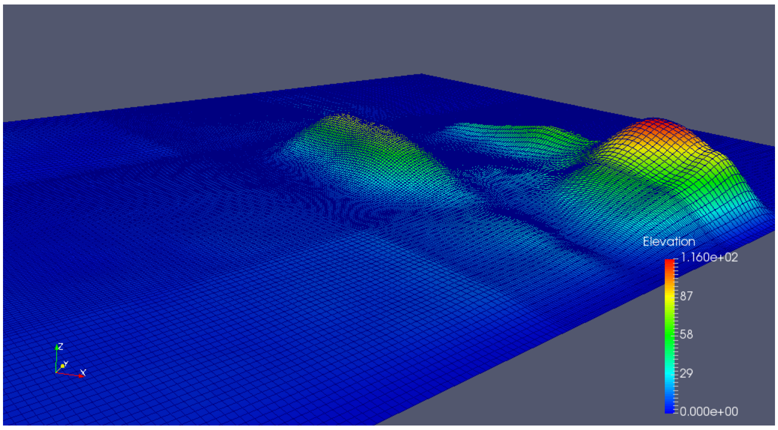

Figure 1. The Digital Elevation Model of Askervein and its surroundings.

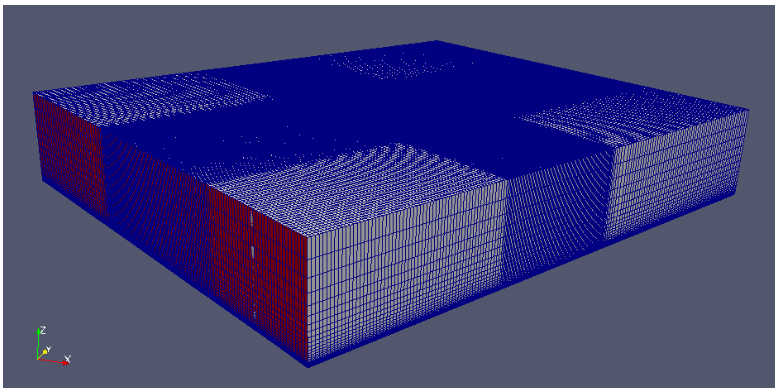

Figure 2. The discretized domain configuration used in the CFD simulations. The bounding box dimensions are 6 km x 5 km x 1.5 km.

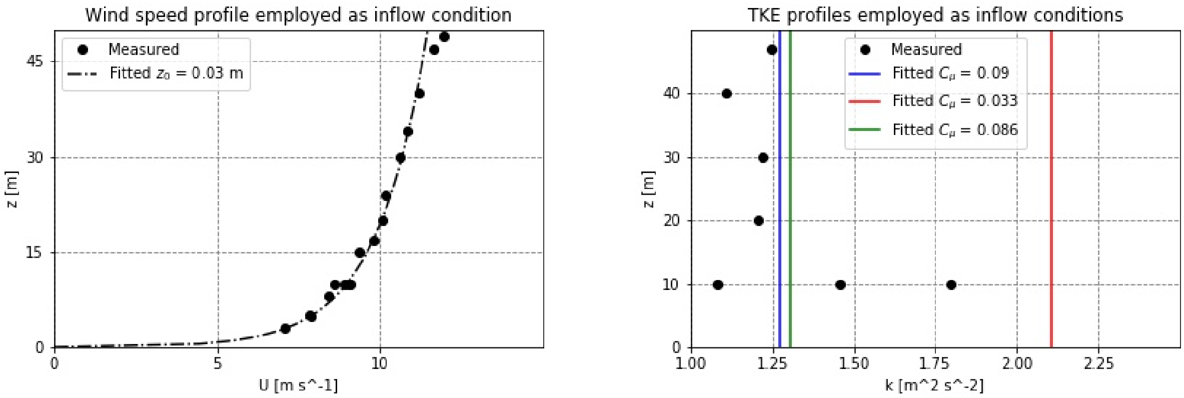

Figure 3. The log-law curve fitted to the measurements which was used as inflow condition in the simulations (left) and TKE profiles (right). The green profile was the only curve actually fitted to the measurements, the others were solely based on turbulence model considerations.

Table 1. Inflow and model parameters used in the simulations

Model	z_0 $[m]$	u^* $[m\ s^{-1}]$	C_μ	σ_ϵ	k_{ref} $[m^2\ s^{-2}]$
Standard	0.03	0.618	0.090	1.300	1.27
Atmospheric	0.03	0.618	0.033	1.835	2.11
Fitted	0.03	0.618	0.086	1.135	1.30

4. RESULTS

The OpenFOAM solver *simpleFoam* was used for all the simulations in this section. It consists of a steady-state, incompressible, turbulent-flow solver which suits the modeling of the neutral ASL. The convection scheme was set as upwind for the U, k and ϵ fields. In what concerns the solvers, the Generalised Geometric-Algebraic Multi-Grid (GAMG) was used for pressure, whilst the Preconditioned Bi-Conjugate Gradient (PBiCG) was employed for the remaining fields. The solver convergence criteria was defined as 1E-4 for all fields with 0.3 relaxation factor for pressure and 0.7 for the remaining fields. The CFD simulations were carried on a desktop computer with 8 4GHz cores and 16GB RAM in parallel. In order to evaluate the grid convergence, four consecutively finer structured meshes were generated, which are summarized in Tab. 2.

The overall behavior of the wind was captured reasonably well by all three models along Line A (10 m above ground level), as can be seen in Fig. 4. The Speed Ratio (SR) approaches the hill with the value of unity, indicating that the inflowing boundary-layer is sustained, and thereafter decreases due to flow deceleration near the hill base. As the wind reaches the top of the hill, the speed-up effect causes great flow acceleration and wind speed increases considerably. Upstream of the hill top, the models employed achieved good agreement with the data, slightly over predicting the SR upstream and under predicting it at the hill top. In the lee of the hill the numerical results deviated substantially from the measurements and overestimated the SR. The Atmospheric model showed better agreement with the data by a slight margin compared to the other models, but still exaggerated the wind speed values.

The TKE behavior was assessed similarly along Line A, which is shown in Fig. 5. The Turbulence Kinetic Energy ratio (TKER) smoothly increased as the hill top was approached upstream, and quickly downstream a slight decrease was followed by a pronounced surge in TKE, which reached nearly four times the reference value. Upstream, the models captured well the TKE and showed a very similar behavior, marginally exceeding the measurements. In the lee all models deviate both the measurements and substantially underestimate the TKER, mainly the Atmospheric model. Also, it appears that downstream the hill top the models become more sensitive to grid discretization and turbulence model coefficient C_μ, which is closely related to the TKE production term, since there is greater spread in the results.

In addition to the mean wind speed and TKE variations at a fixed height above ground, it is also necessary to evaluate the wind shear in those fields at the hill top to better characterize the wind climate near Askervein Hill. The SR profiles at the hill top, shown in Fig. 6, were calculated with a height-dependent reference speed $U_{ref}(z)$ and not a fixed value, both for the measurements and simulations. Altogether, the models underestimated the SR. The deviation was more accentuated near the ground, where the SR was found to be nearly 25 % smaller than the data, and then smoothly decreased until it became negligible. Above 30 m, all models showed solid agreement with the data and virtually behaved equally. It can also be observed that, although the models showed analogous performance at all heights, there was found substantial difference between consecutive grids. The coarser meshes negatively distort the results near the ground since the height of the first grid cell above ground (5 and 2.5 m) scales up with the height at which some of the measurements were performed. Grid convergence was found between grids M3 and M4, highlighting the importance of the grid resolution near ground.

Similarly, the TKER profiles were also analyzed at the hill top and are shown in Fig. 7. In this case, the reference value k_{ref} for the data is constant and set as the mean TKE at the reference site and for the simulations as the TKE at the inlet. Regarding the data, it can be observed that the TKE is greater than at the reference site at all heights, displaying a steep peak below 10 m. Above 10 m, the TKER profile appears to be constant with height despite the lack of measurements between 10 m and 40 m. Near the ground it seems unanimous that the models tend to under predict the TKER when finer grids are employed, whereas coarser grids display much better agreement with the measurements. This figure shows once again the sensitivity of the models to the grid resolution near the terrain surface, where gradients are high and wall-functions are used.

In order to evaluate the overall model performance, there were established an assessment metric based on the Hit Rate (HR) and Relative Error (ϵ). The former assigns the value of unity if the simulated value is within one standard deviation from the measurement, else it assigns the value zero. If the standard deviation is absent, which is the case of the TKE, the window considered is 25 % of the measured value. As for the latter, it is simply the relative difference between the simulated and the measured value, using the measurement as reference. The performance of each simulated case is summarized in Tab. 3.

It should be emphasized that only the measurements along line A were considered for the metrics, which are Figs. 4 and 5. As can be seen, the Atmospheric models achieved the best results amongst the evaluated propositions, displaying worst results only for the maximum TKER error $\epsilon_{k,max}$. Standard and Fitted models performed much alike, which is to be expected since their constants C_μ are very close. It should also be noted that despite the fact that all propositions shown high Hit Rates ($> 70\%$), the considerable deviations from the measurements are captured by the relative errors (20% on average).

Table 2. Numerical grids employed in the sensitivity analysis

Mesh	Volumes	n_x	n_y	n_z	ΔZ_w^* $[m]$	Domain Size [km]
M1	1,152,000	200	160	36	5.0	6 x 5 x 1.5
M2	2,064,860	245	196	43	2.5	6 x 5 x 1.5
M3	3,744,000	300	240	52	1.0	6 x 5 x 1.5
M4	5,713,200	345	276	60	0.5	6 x 5 x 1.5

*Height of the first cell above ground.

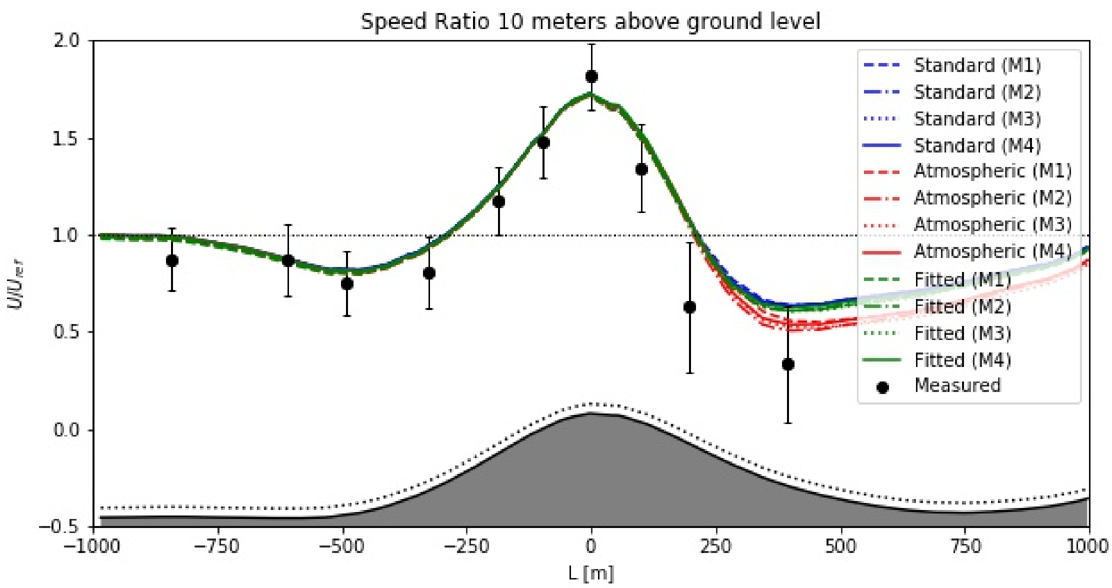

Figure 4. Speed ratio along line A 10 meters above ground level.

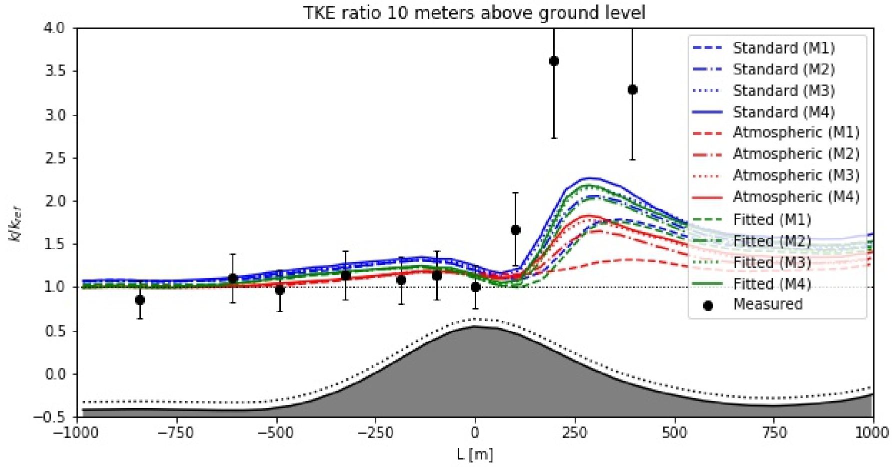

Figure 5. TKE ratio along line A 10 meters above ground level. The error bar in measurements denote the 25 % criterion for the Hit Rate.

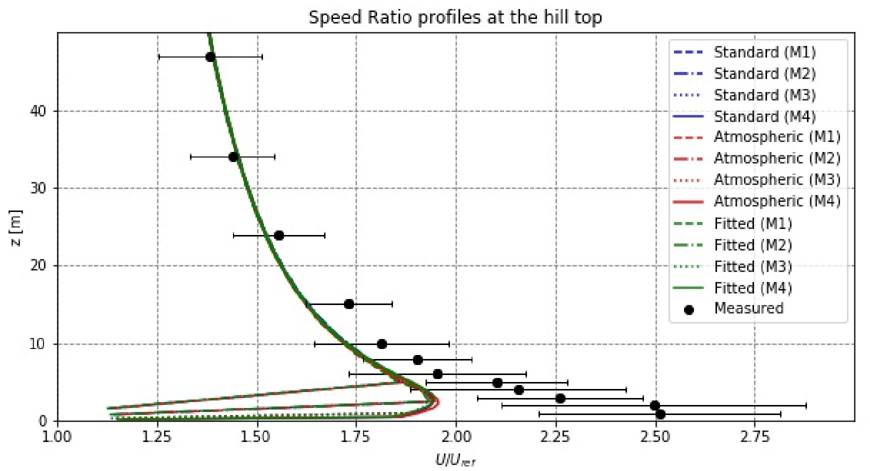

Figure 6. Speed ratio profiles at the hill top.

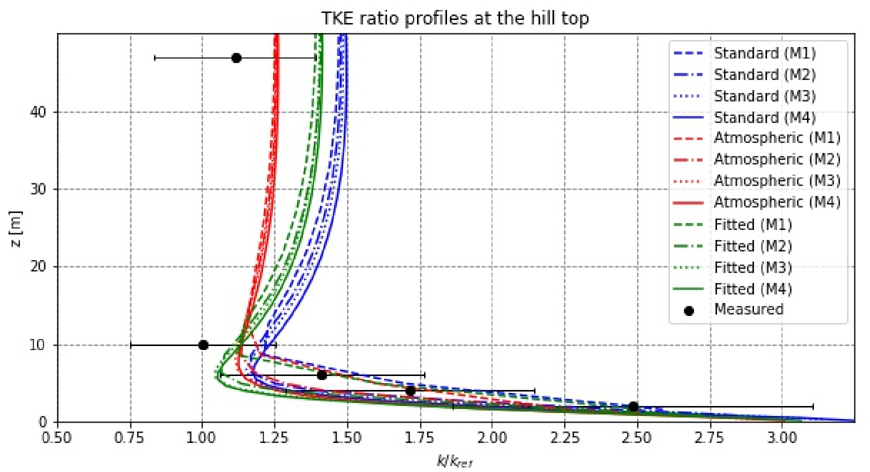

Figure 7. TKE ratio profiles at the hill top. The error bar in measurements denote the arbitraty 25 % criterion for the Hit Rate.

Table 3. Hit rates and relative errors for the simulated cases

Model	HR_U [%]	e_U [%]	$e_{U,max}$ [%]	HR_k [%]	e_k [%]	$e_{k,max}$ [%]
Standard (M1)	80	22	90	60	24	64
Standard (M2)	80	22	89	70	23	54
Standard (M3)	80	22	90	70	22	50
Standard (M4)	90	22	89	60	23	48
Atmospheric (M1)	90	19	70	70	22	67
Atmospheric (M2)	90	17	65	70	20	62
Atmospheric (M3)	90	18	69	70	19	58
Atmospheric (M4)	90	19	71	70	19	57
Fitted (M1)	90	21	82	70	22	66
Fitted (M2)	90	21	81	70	20	56
Fitted (M3)	90	21	81	70	20	52
Fitted (M4)	90	22	86	70	20	51

5. CONCLUSIONS

In this paper, the wind flow over Askervein hill was simulated with a consistent combination of turbulence model, wall-functions and inflow conditions by using the C++ toolbox OpenFOAM. A number of grids and $k - \epsilon$ model constants were used so as to evaluate the sensitivity to the inputs and determine the best set-up.

Among the three evaluated propositions, namely the Standard, Atmospheric and Fitted, they generally captured well the flow behavior near the hill but the lee region. There, significant deviations from the data appeared and the models generally overestimated the wind speed whilst considerably underestimated the TKE. In addition, the results shown that closer to the ground and near the wake of Askervein the models became more sensitive to grid refinement, mainly for the TKE field. Results ceased changing considerably between grid M3 and M4, which suggests the mesh convergence is near and for the purpose of sensitivity analysis it was considered enough.

In conclusion, even though there was found substantial deviations from the measurements, it should be noted that the heights assessed are considerably smaller than the hub heights of utility scale wind turbines, which are of the order of 100 m. In addition, the wind energy production is estimated based on the wind speed and not TKE, which deviated more pronouncedly from the measurements.

6. ACKNOWLEDGEMENTS

The authors would kindly like to thank Taylor and Teunissen (1987) for the data provided from the Askervein hill project, and also to the Brazilian National Council for Scientific and Technological Development (CNPq).

7. REFERENCES

Balogh, M., Parente, A. and Benocci, C., 2012. “Rans simulation of abl flow over complex terrains applying an enhanced $k - \epsilon$ model and wall function formulation: Implementation and comparison for fluent and openfoam”. *Journal of Wind Engineering and Industrial Aerodynamics*, Vol. 104-106, pp. 360–368.

Beljaars, A.C.M., Walmsley, J.L. and Taylor, P.A., 1987. “A mixed spectral finite-difference model for neutrally stratified boundary-layer flow over roughness changes and topography”. *Boundary-Layer Meteorology*, Vol. 38, pp. 273–303.

Castro, F.A., Palma, J.M.L.M. and Lopes, A.S., 2003. “Simulation of the askervein flow. part 1: Reynolds averaged navierâĂŞstokes equations (k-epsilon turbulence model)”. *Boundary Layer Meteorology*, Vol. 107, pp. 501–530.

Jackson, P.S. and Hunt, J.C.R., 1975. “Turbulent windflow over a low hill”. *Quarterly Journal of the Royal Meteorology Society*, Vol. 101, pp. 929–955.

Parente, A., GorlÃl’, C., van Beeck, J. and Benocci, C., 2011. “Improved $k - \epsilon$ model and wall function formulation for the rans simulation of abl flows”. *Journal of Wind Engineering and Industrial Aerodynamics*, Vol. 99, pp. 267–278.

Richards, P.J. and Hoxey, R., 1993. “Appropriate boundary conditions for computational wind engineering models using the $k - \epsilon$ turbulence model”. *Journal of Wind Engineering and Industrial Aerodynamics*, Vol. 47, pp. 145–153.

Richards, P.J. and Norris, S.E., 2011. “Appropriate boundary conditions for computational wind engineering models revisited”. *Journal of Wind Engineering and Industrial Aerodynamics*, Vol. 99, pp. 257–266.

Schmidt, J., Peralta, C. and Stoevesandt, B., 2012. “Automated generation of structured meshes for wind energy applications”. In *Open Source CFD International Conference*. London, United Kingdom.

Stull, R., 2017. *Practical Meteorology: An Algebra-based Survey of Atmospheric Science*. University of British Columbia, 1st edition.

Taylor, P.A. and Teunissen, H.W., 1987. "The askervein hill project: overview and background data". *Boundary-Layer Meteorology*, Vol. 39, pp. 15–39.

8. RESPONSIBILITY NOTICE

The authors are the only responsible for the printed material included in this paper.